

Modeling a Combined Photovoltaic-Thermal Solar Panel

Bradley J. Fontenault¹ and Ernesto Gutierrez-Miravete^{2,*}

¹General Dynamics Electric Boat Corporation, ²Rensselaer Polytechnic Institute

* Corresponding Author: RPI, 275 Windsor Street, Hartford, CT 06120; gutiee@rpi.edu

Abstract: The electrical efficiency of a photovoltaic (PV) cell decreases as its temperature increases. Since PV cells must be arranged in direct sunlight to produce electricity, heating is inevitable. A heat exchanger can be adapted to a PV cell to extract heat and hence increase the conversion efficiency while using heat absorbed from the cells for secondary applications. The thermal system consists of a rectangular aluminum reservoir that is mounted to the backside of PV panels, through which water flows. Analysis of the proposed photovoltaic-thermal (PV/T) solar panel design was performed using COMSOL Multiphysics software. Combinations of water flow rates and reservoir thicknesses were analyzed to determine which produced optimal PV/T total efficiencies. Higher total panel efficiencies (additive efficiency of thermal and electrical efficiencies) were achieved in configurations utilizing the highest flow rates and largest reservoir thickness. However, elevated flow rates translated to minimal net temperature differences between the PV/T panel inlet and outlet.

Keywords: Photovoltaic, Thermal, Solar Panel, COMSOL, Efficiency

1. Introduction

Global warming, rising fuel oil prices, and other environmental factors in the world today are influencing organizations in the energy industry to develop green energy technologies to be used in both commercial and residential markets. One such technology was invented in 1894 by Charles Fritts and is referred to as the PV cell [1]. PV cells convert sunlight into electrical energy, which can be harnessed and supplied to the electrical grid. The first PV cell created by Fritts was only 1% efficient; however, modern day single junction solar cells have efficiencies up to 23% [2]. New PV technologies have been shown to improve energy utilization efficiency, such as multi-junction cells, optical frequency shifting, and concentrated photovoltaic (CPV) systems, among others; however, these technologies are expensive both

in acquisition and maintenance costs and resultantly have not been utilized on a wide scale at this time [3].

In commercial and residential applications, PV cells are assembled into modules, which are then assembled into panels. PV panels are then assembled to form arrays. The most applicable regions to use PV panels are in environments with plentiful amounts of sun exposure, which most often are regions with warm climates.

PV panel surface temperatures increase due to low solar energy-to-electricity efficiencies as not all energy absorbed by PV cells can be converted to electrical energy. To satisfy the law of conservation of energy, the remaining solar energy must be converted to heat. PV cell efficiency is further reduced when installed in environments with warm climates (i.e. high ambient temperatures), as heat dissipation from the panels is reduced. Therefore, it is relevant to develop methods of cooling the PV cells to increase output efficiency. Oh et al. [4] has found that poorly ventilated PV panels in environments with high ambient temperatures can reach temperatures greater than 90 degrees Celsius. These conditions are not only dangerous, but also reduce panel efficiency and service life.

Both active and passive methods of cooling PV panels have been researched and analyzed to date. From these studies it has been concluded that controlling the temperature increase of PV panels results in gains in electrical output of the panels. In many of these investigations, the thermal energy extracted from the PV panels has been utilized for a variety of low temperature applications (i.e. residential water heating, radiant floor heating, swimming pool heating, etc.). These systems are referred to as hybrid photovoltaic and thermal (PV/T) systems. Teo et al. [5] investigated an active PV panel cooling system, in which the PV panels were cooled by forced convection, with air being the heat carrying fluid. This system yielded a 4-5% electrical efficiency increase. Chen et al. [6]

developed a hybrid PV/heat pump system using refrigerant fluid R134a as the heat carrying fluid. The coefficient of performance (COP) of the heat pump and electrical efficiency of the PV panel was measured at different condensing fluid flow rates and temperatures.

Practical applications of PV/T systems have been installed recently throughout the United States. The largest PV/T solar panel installation in the United States was brought online in February 2012 in Rhode Island at Brown University's Katherine Moran Coleman Aquatics Center. In this application, 168-patented PV/T panels were installed on the center's roof, which under full sun exposure can provide enough electricity to light the building and heat the one million gallon swimming pool inside of it [7].

Yang et al. [3] developed a functionally graded material (FGM) with copper water pipes cast into it that was bonded with thermal paste to the backside of a PV/T panel. Cooling water was pumped at various flow rates through the cast copper pipes to decrease the PV/T panel temperature thus increasing PV/T panel electrical efficiency by up to 2%. This study also analyzed the thermal efficiency of the FGM/copper tube design and reported that a combined thermal and electrical efficiency of 71% could be achieved, compared to 53-68% total efficiency of other PV/T concepts.

The study presented in this report leverages off work previously accomplished by Yang et al. [3], by utilizing the identical PV/T panel and thermal glue properties. A thin rectangular reservoir through which water will flow through and carry heat away from the panel will be analyzed as shown in Figure 1 in lieu of the copper pipe-FGM design. This is accomplished in the COMSOL Multiphysics finite element software package. Increases in electrical efficiency of the panel at various operating temperatures will be calculated from the PV cell thermal coefficient.

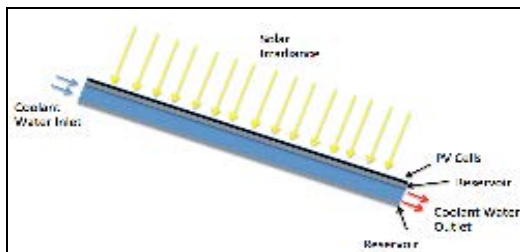


Figure 1: Conceptual PV/T design analyzed in this study

2. Methodology/Approach

In this project, a single PV/T panel will be evaluated using COMSOL Multiphysics FEA software, from which results could be extrapolated for an array of identical PV/T panels. An aluminum reservoir will be modeled in COMSOL for the subject PV/T panel, through which water at a predetermined inlet temperature will flow. Three different reservoir thicknesses will be analyzed to determine the impact they have on cooling the panel. As this study investigates forced convection using water as the coolant, or heat carrying fluid, various water flow rates will also be analyzed for impact to cooling performance.

2.1 PV/T Test Model and Arrangement

Work being done in this study will utilize the PV materials defined in the work done by Yang et al. [3], and will use the uncooled PV/T panel data as a reference point since an experimental analysis of the subject PV/T design was not feasible for this project. The PV cells making up the PV panel assemble into an approximate length, width, and thickness of 30.5 cm X 30.5 cm X 0.27 mm, respectively. For simplicity, it is assumed that the whole panel is covered in PV cells, with no packing material (material used to fill in gaps between the cells on a panel). The PV cells are commercial grade monocrystalline silicon cells with electrical efficiency, $\eta_{T_{ref}}$, of 13% and have a thermal coefficient, $\beta_{T_{ref}}$, of 0.54% [1/K] [3]. The thermal coefficient represents the degradation of PV cell output per degree of temperature increase.

The cooling reservoir is bond to the back of the panel by a thermal paste with an approximate uniform thickness of 0.3 mm over the whole surface area of the reservoir – PV panel interface. The reservoir walls are approximately 1 mm in thickness and are constructed from aluminum. Aluminum was chosen as the reservoir enclosure material, due to its high thermal conductivity, which promotes heat transfer across its boundary, its availability, and its relatively low cost in comparison to other conductive metals such as copper. A cross section view of the assembly is shown below in Figure 2. It is assumed that the conceptual PV/T

panel being considered in this project is not coated with a protective glass and/or a layer(s) of ethylene vinyl-acetate (EVA), both of which are typically used to protect PV cells in real world applications. However, while protecting the delicate silicon PV panels, these encapsulation materials hinder the performance of PV panels by affecting the panel's absorptivity of solar irradiance. Teo et al. [5] found that the highest temperatures experienced in a PV panel are on the backside of the panel due to the high thermal conductivity of the silicon PV material; therefore, precedence exists for cooling the panel from the backside rather than using water to cool the panel on the topside.

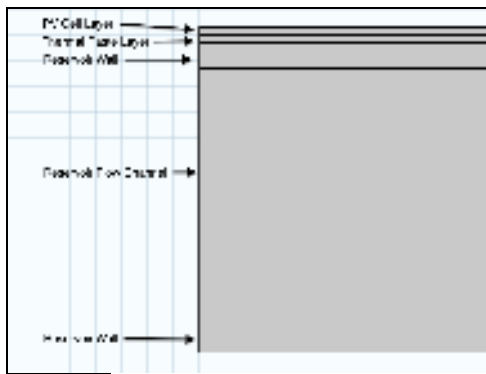


Figure 2: PV/T solar panel simulation test set-up

2.2 PV/T Panel Model Assumptions

Several assumptions must be made to perform this study regarding the conceptual PV/T panel construction, atmospheric conditions, water flow characteristics, and other factors, which impact this thermal analysis.

1. The solar irradiance imparted on the entire surface of the PV/T panel is 1000 W/m².
2. All solar irradiance that is not used to produce electricity in the PV/T panel will be developed into heat.
3. The subject conceptual PV/T panel is not constructed with a glass and/or EVA encapsulating layer, which would result in decreased PV/T absorption of solar irradiance.
4. No dust or any other agent is deposited on the PV/T surface affecting the absorptivity of the PV/T panel.
5. The coolant water at the inlet of the conceptual PV/T reservoir will have uniform temperature.

6. The flow through the coolant reservoir is considered to be fully laminar and incompressible.

7. The ambient temperature surrounding the PV/T panel is 298.15 K.

8. An average wind speed of 1 m/s exists throughout the simulations.

2.3 Theory and Governing Equations

All three modes of heat transfer are involved when considering a basic PV panel. Heat is transferred within the PV cell and its structure by conduction and heat is transferred to the PV/T panel surroundings by both free and forced convection. Heat is also removed from the panel in the form of long-wave radiation [8]. Heat transfer by conduction to the panel structural framework is often ignored due to the small area of contact points; however, it will be considered throughout the COMSOL simulations from the PV/T panel surface and through the reservoir casing. Steady state heat conduction through from the PV/T cell surface to the reservoir enclosure casing is given by Equation [1] below.

$$\nabla \cdot (k\nabla T) = 0 \quad [1]$$

The PV panel shown in Figure 1 receives energy from the solar irradiance, converts some of it into electricity through the PV effect and the rest is transformed into heat. The objective of attaching the thermal panel underneath the PV cell is to remove as much as this heat as possible in order to increase the efficiency. The heat loss due to forced convection on the top and bottom surfaces of a PV cell is given by Equation [2] below [8].

$$q_{conv} = -h_{c,forced} \cdot A \cdot (T_{pv} - T_{amb}) \quad [2]$$

The total convective heat transfer is a combination of the heat transfer at the top and bottom surfaces of the PV/T panel and the heat transfer from the flowing water in the reservoir. The FEA software being used in this study, COMSOL, contains a non-isothermal laminar flow and conjugate heat transfer physics module, which was used to model conduction heat transport within the cell as well as the convective heat transfer in the water reservoir on the backside of the PV panel. This package is appropriate for this study, because of the inhomogeneous temperature field that is created as water flows from the inlet to the outlet of the reservoir. COMSOL numerically solves the

continuity and momentum equations, which are the governing equations for the fluid flow, and are shown below in Equations [3] and [4], respectively [9].

$$\nabla \cdot (\rho u) = 0 \quad [3]$$

$$\rho u \cdot \nabla u = -\nabla p + \nabla \cdot \left(\mu \left(\nabla u + (\nabla u)^T \right) \right) \quad [4]$$

The conduction-convection equation is also solved for the heat transfer in the flowing water, which is shown in Equation [5].

$$\rho C_p u \cdot \nabla T = \nabla \cdot (k \nabla T) \quad [5]$$

The longwave radiation heat loss can be calculated from Equation [6] below [8].

$$q_{lw} = \varepsilon \cdot \sigma \cdot (T_{pv}^4 - T_{amb}^4) \quad [6]$$

The thermal model analyzed in this study is similar to that modeled by Jones and Underwood [8], although the amount of energy applied to the PV cell that is converted to heat energy is calculated using the method of Kerzmann and Schaefer [10]. The amount of energy converting into electric power in the PV cell is a function of the PV cell efficiency, η_{pv} , as shown below in Equation [7], which satisfies Assumption 2 above.

$$q_{heat}^* = q_{rad}^* \cdot (1 - \eta_{pv}) \quad [7]$$

The PV cell electrical efficiency, η_{pv} , is given by Equation [8] below as a function of its efficiency at reference temperature, the PV cell temperature, and the PV cell thermal coefficient [14].

$$\eta_{pv} = \eta_{T_{ref}} \left[1 - \beta_{ref} (T_{pv} - T_{ref}) \right] \quad [8]$$

The PV cell electrical output efficiency can also be expressed as a function of PV cell power output, solar irradiance, and the PV cell surface area as shown in Equation [9] below [5].

$$\eta_{pv} = \frac{V_{mp} I_{mp}}{q_{rad}^* A} \quad [9]$$

In Equation [8], $\eta_{T_{ref}}$, is the PV cell efficiency at reference conditions (i.e. $T_{ref} = 25^\circ C$, $q_{rad}^* = 1000 \frac{W}{m^2}$), and β_{ref} is the PV thermal coefficient.

2.4 Test Cases

Numerous test cases were simulated in COMSOL, in which water inlet velocity and reservoir thickness were varied to determine optimal design conditions for the PV/T system. A summary of the test cases selected in this study is shown in Table 1 below. A constant ambient temperature of 298.15 K was used for all test cases to simulate laboratory test conditions and to concentrate the focus on performance impacts due to variability of flow rate and reservoir thickness. For each test case, the flow was confirmed to be laminar by confirming that the dimensionless Reynolds number, Re, was less than 2300 to satisfy Assumption 6.

A value of 6.5 W/(m²K) was used for the forced convection heat transfer coefficient for convection occurring at the top and bottom surfaces of the PV/T panel. This value correlates to the average heat transfer coefficient value sourced by Jones and Underwood [8], for a panel subjected to wind speeds of 1 m/s, which satisfies Assumption 8 above.

The materials used to construct and analyze the conceptual PV/T system shown above in Figure 2, consist of silicon, silicone thermal paste, aluminum, and water for the PV/T cell, thermal paste, reservoir enclosure, and coolant fluid, respectively. Values for all material properties except for the silicone thermal paste were provided by COMSOL at each time step in the simulations, including temperature dependent properties for water. The material property values for the thermal paste were obtained from Yang et al. [3].

Table 1: Summary of test cases

Test Number	Water Temperature at Inlet, T _{in} (K)	Flow Channel Length (m)	Flow Channel Thickness (m)	Dh (m)	U _{inlet} (m/s)	v (m ³ /s)	Re	Laminar (Re < 2300)
1a	298.15	0.305	0.015	0.03	0.0002	9.14E-07	6.57	Yes
2a	298.15	0.305	0.01	0.02	0.0002	9.14E-07	4.38	Yes
3a	298.15	0.305	0.005	0.01	0.0002	9.14E-07	2.19	Yes
1b	298.15	0.305	0.015	0.03	0.001	9.14E-07	32.83	Yes
2b	298.15	0.305	0.01	0.02	0.001	9.14E-07	21.89	Yes
3b	298.15	0.305	0.005	0.01	0.001	9.14E-07	10.94	Yes
1c	298.15	0.305	0.015	0.03	0.005	9.14E-07	164.17	Yes
2c	298.15	0.305	0.01	0.02	0.005	9.14E-07	109.45	Yes
3c	298.15	0.305	0.005	0.01	0.005	9.14E-07	54.72	Yes
1d	298.15	0.305	0.015	0.03	0.01	9.14E-07	328.34	Yes
2d	298.15	0.305	0.01	0.02	0.01	9.14E-07	218.89	Yes
3d	298.15	0.305	0.005	0.01	0.01	9.14E-07	109.45	Yes

2.5 Solving

COMSOL Multiphysics was used to simulate and solve the flow and heat transfer model described thus far using various equations defined in Section 2.2 of this paper. All of the

simulations run were steady state studies solved in two dimensions, in which the conjugate heat transfer and laminar flow physics modules were utilized. It was verified that all the flow velocities used would produce laminar flows, rather than turbulent flows, by calculating the Reynolds number, Re. For this study, the flow in the channel can be characterized by flow between parallel planes, in which the hydraulic diameter, D_h , becomes twice the plate spacing [11].

The software modeled the flow through the PV/T reservoir by solving the continuity, momentum, and energy equations. At each iteration in the simulations performed, the PV cell efficiency, η_{pv} , is calculated from Equation [8] from the user input values for β_{ref} , $\eta_{T_{ref}}$, T_{ref} , and from the COMSOL solved value for the cell temperature, T_{pv} . The amount of solar irradiance, q_{rad}'' , that transforms into heat, q_{heat}'' , is then calculated from Equation [7]. Values for the thermal efficiency of the cell were calculated iteratively by COMSOL using Equations [10] - [12] below. Convergence of the steady state solution was monitored throughout the simulation, resulting in 30-40 second (real time) convergence times using the normal physics controlled mesh sequence setting (yields approximately 15,240 elements).

To calculate the thermal efficiency of the panel, first, the total amount of energy (solar irradiance) into the cell must be calculated, as well as the thermal energy extracted by the coolant water, which is given by Equations [10] and [11] below.

$$E_{in} = q_{rad}'' \cdot A \quad [10]$$

$$E_{water} = \dot{m}_{water} C_{p_{water}} (T_{out} - T_{in}) \quad [11]$$

The thermal efficiency is simply given by Equation [14].

$$\eta_{th} = \frac{E_{water}}{E_{in}} \quad [12]$$

Similarly, the quantity of the total input energy converted to electrical energy can be approximated from the solution data by obtaining the average electrical efficiency of the PV/T panel, and multiplying it by the total energy into the panel. The electrical efficiency was calculated in COMSOL each iteration in the simulations by Equation [8] from which an

average of the efficiency for the entire PV cell was obtained at the completion of the simulation. This is shown by Equation [14].

$$E_{pv} = \bar{\eta}_{pv} \cdot E_{in} \quad [13]$$

A total efficiency of the cell was then calculated by Equation [14].

$$\eta_{tot} = \frac{(E_{water} + E_{pv})}{E_{in}} \quad [14]$$

3. Results and Discussion

The simulations performed assumed that the water inlet temperature was of uniform temperature equal to 298.15 K (25 °C), which is the same temperature specified for the ambient temperature. This water temperature was chosen to imitate a scenario in which the cooling water may reach ambient air temperature before entering the cooling reservoir to carry heat away from the PV/T panel. For the remainder of this paper, flow reservoir thickness and flow channel thickness are to be considered interchangeable terms.

In Figure 3, the velocity profile of the water in the flow channel is shown. A similar laminar flow profile was achieved in each of the test cases and is only shown once here for information. One can see the no-slip boundary condition invoked on the interior walls of the reservoir, and the parabolic flow profile that is created.

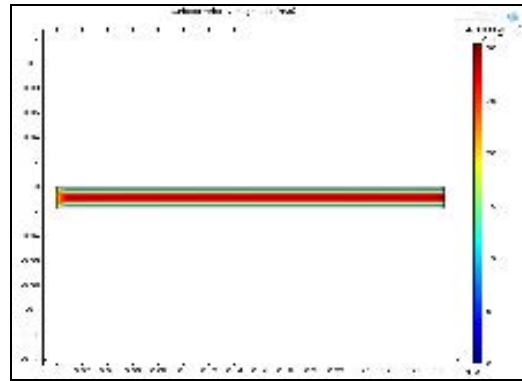


Figure 3: Laminar flow profile common to all test cases

In Figure 4 below, a two-dimensional plot for the steady state solution of the temperature distribution for test case 1a is shown. The temperature distribution shown was typical of all the test cases; however, it was found that the

greater the flow channel thickness at low flow velocities, the cooler the system remains.

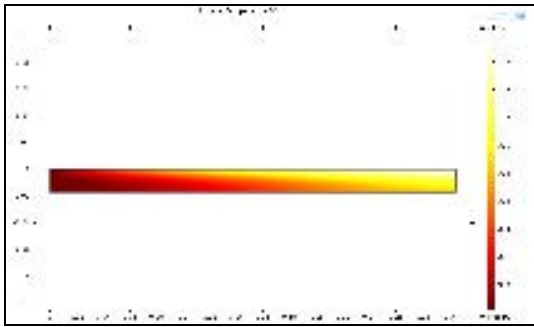


Figure 4: Test Case “1a” two-dimensional surface plot of temperature at steady-state

In Figure 5, the temperature gradient across the PV/T system is shown for a high flow velocity test case. In comparison to Figure 4, the effect velocity has on the temperature gradient of the cooling water is evident.

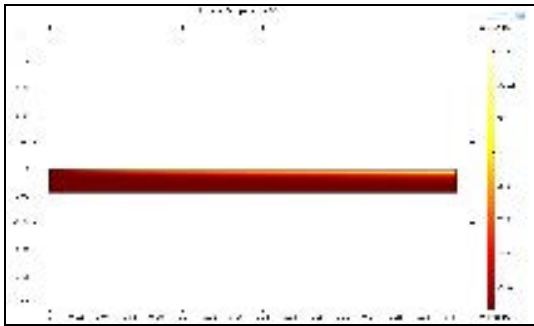


Figure 5: Test Case “1d” two-dimensional surface plot of temperature at steady state

This phenomenon is shown further by visual inspection of the raw data extracted from the COMSOL solutions to develop Figure 6. In Figure 6, the surface temperature of the PV/T panel is plotted against inlet water velocity for Test Cases “1a” through “3d”. It can be inferred that the higher the cooling water velocity, the lower the average PV/T surface temperature will be. As the water temperature increases in the reservoir, the difference in temperature between the PV/T panel surface and the water decreases, resulting in decreased heat transfer across the reservoir-thermal paste interface.

At the highest flow velocity examined, the PV/T surface temperature actually reaches the lowest temperature when the narrowest reservoir is utilized. It is also shown that the largest flow channels at high velocities result in higher average surface temperatures, whereas the

highest surface temperatures at lower flow rates are obtained using the smallest flow channel. This is due to the physical mass of water in the channel and the amount of time it remains in the channel (i.e. mass flow rate) to absorb heat.

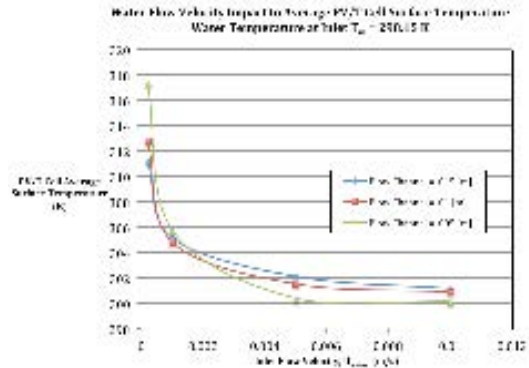


Figure 6: Water velocity impact to average PV/T cell surface temperature

In terms of cell electrical output efficiency, the cooler the PV/T surface is, the greater the efficiency will be, which is shown in Figure 7. As previously mentioned, the smallest reservoir thickness at the high inlet velocity results in the lowest average PV/T surface temperature, thus the highest PV/T output efficiency of approximately 12.9%, which approaches the NTOC PV output efficiency of 13%. It should be noted, however, that the difference in cell efficiency and surface temperature at the three higher flow velocities is minor, and a significant difference is only given at the lowest flow velocity of 0.0002 m/s.

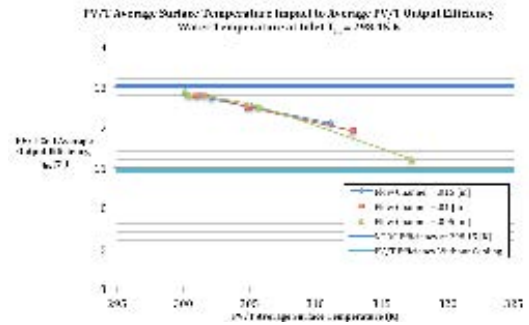


Figure 7: PV/T average surface temperature impact to average PV/T output efficiency

A similar trend for the PV/T surface temperature shown in Figure 6 is displayed in Figure 8 for the cooling water outlet temperature. For low water flow velocities and narrow reservoir thicknesses, the outlet temperature is much warmer than for larger flow channels. This is due to the larger volume of fluid in the

thicker reservoirs, which naturally heats up slower than the smaller volume in the narrower reservoirs. However, at high velocities the outlet temperature for the narrower flow thickness is slightly cooler than the largest flow thicknesses, although the temperature of the fluid hardly increases from inlet temperature.

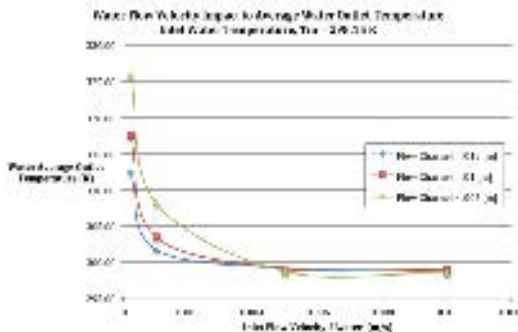


Figure 8: Water flow velocity impact to average water outlet temperature

In Figure 9 the combined efficiency of the PV/T panel is plotted with respect to the inlet flow velocity, which shows that the largest reservoir thickness, combined with the highest flow velocity is the most efficient option with a water inlet temperature equivalent to the ambient temperature of 298.15 K. As mentioned previously, however, this option does not result in an optimal water outlet temperature that would be useful for a secondary application, such as heating potable water, heating a swimming pool, or other functions. All options, except for the smallest flow channel at the lowest flow velocity, yield a measurable gain in PV/T electrical output efficiency.

Also worth noting is the relatively high thermal efficiency of the 0.01 m and 0.015 m flow channel configurations at higher water flow velocities. This is mainly due to Assumptions 1 - 4 stated in Section 2.2.1 and the extreme sensitivity of thermal efficiency to temperature change at high flow velocities. It was conservative to assume that all solar irradiance energy not converted to electrical energy would be developed into heat. It is reasonable to consider that a functional PV/T panel would not absorb a percentage of the solar irradiance imparted on the panel due to the fact some of the solar irradiance is of the incorrect wavelength for any given PV cell material. Also, the surface of the PV/T panel would likely get dirty or dusty over time, which would impact the absorptivity of the panel. Therefore, a proportional reduction

in thermal efficiency could be expected with a decrease in the absorptivity of the panel.

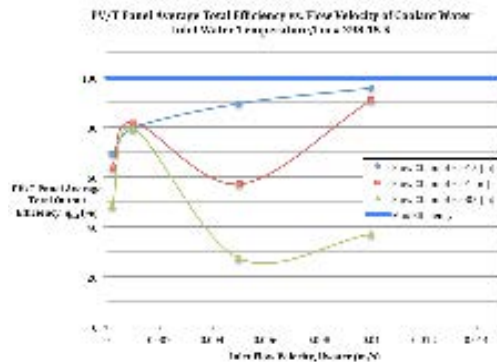


Figure 9: PV/T panel average total efficiency vs. flow velocity of coolant water

The thermal efficiency of the PV/T panel at high flow velocities was found to be extremely sensitive with calculated values of the difference in water temperature at the inlet and outlet of the panel. The average temperature calculated in COMSOL was used to determine the thermal efficiency of the panel. Using Equation [12], it was found that at the highest flow velocity evaluated (0.01 m/s) and largest flow channel thickness (0.015 m), variations in the outlet temperature as small as 0.1 K resulted in a 20% difference in thermal efficiency.

4. Conclusions

In this work, a conceptual PV/T design was modeled and analyzed using a commercial finite element software package, COMSOL Multiphysics: Version 4.2a. The PV/T panel evaluated consisted of monocrystalline silicon PV cells that were bound with a silicone thermal paste to an aluminum reservoir through which coolant water flowed. Numerous simulations were completed to model the heat transfer across the PV/T panel and ultimately to determine the PV/T electrical output and thermal efficiencies of the panel. Water flow velocity and flow channel thickness were varied and analyzed to determine which combinations yielded not only the highest total PV/T efficiency, but also the most useful thermal and electrical output.

It was found that the highest total PV/T panel efficiencies were achieved for test cases involving combinations of high flow velocity and large flow channel thicknesses. The highest total cell efficiency obtained of 95.7% was

obtained from Test Case “1d”, in which the flow thickness was 0.015 m and the inlet flow velocity was 0.01 m/s. Test Case “3c” was found to be the least efficient configuration, which recorded a total efficiency of 27.5% and consisted of a flow channel thickness of 0.005 m and inlet flow velocity of 0.005 m/s. The highest efficiency obtained is unrealistic, which is due conservative assumptions and the extreme sensitivity of thermal efficiency to temperature change at high water flow velocities. It was deduced that at high flow velocities (i.e. high mass flow rates), slight changes in temperature result in drastic differences in thermal efficiency; therefore, precise temperature measurement is essential for accurate results.

It was also concluded that the PV/T system with the highest efficiency is most likely not the most desirable configuration for practical use. Although high inlet velocities result in the lowest PV/T surface temperatures, thus the highest electrical efficiency, the coolant water exiting the panel experiences no significant temperature change. Therefore, it would not be entirely beneficial to utilize the water exiting the PV/T panel for any practical application. Also, high flow velocities would require larger pumps and more electrical power to operate them depending on the size of the PV/T panel array, which may reduce or negate the electrical gains experienced in such a system. A cost savings study would be required to determine the optimal balance of electrical efficiency and thermal efficiency; however, that is beyond the scope of this study. Future study of this PV/T system could include work evaluating the performance of this system in different climates, utilization of different coolant fluids, and evaluation of various inlet water temperatures.

5. References

- [1] Nelson, Jenny. *The Physics of Solar Cells*. London: Imperial College Press, 2003.
- [2] Turner, Wayne and Steve Doty. *Energy Management Handbook: Sixth Edition*. Lilburn: The Fairmont Press, 2007.
- [3] D. J. Yang, Z. F. Yuan, P. H. Lee, and H. M. Yin, Simulation and experimental validation of heat transfer in a novel hybrid solar panel, *International Journal of Heat and Mass Transfer*, **55**, 1076-1082 (2012)

- [4] Jaewon Oh, Govinda Samy, and Tamizh Mani, Temperature Testing and Analysis of PV Modules Per ANSI/UL 1703 and IEC 61730 Standards, *Conference Record of the IEEE Photovoltaic Specialists Conference, Program - 35th IEEE Photovoltaic Specialists Conference, PVSC 2010*, p 984-988, (2010)
- [5] H. G. Teo, P. S. Lee, and M. N. A. Hawlader, An active cooling system for photovoltaic modules, *Applied Energy*, **90**, 309-315, (2012)
- [6] H. Chen, Saffa B. Riffat, Yu Fu, Experimental study on a hybrid photovoltaic/heat pump system, *Applied Thermal Engineering*, **31**, 4132-4138 (2011)
- [7] Sharp, Rowan, Brown’s Hybrid Solar Panels a First for RI, *Eco RI News: Rhode Island’s Environmental News Source*, 26 February 2012, www.ecoRI.org
- [8] A.D. Jones and C.P. Underwood, A Thermal Model For Photovoltaic Systems, *Solar Energy*, **70**, 349-359 (2001)
- [9] R. Byron Bird, Warren E. Stewart, and Edwin N. Lightfoot, *Transport Phenomena: Second Edition*, New York: John Wiley and Sons, Inc., 2007.
- [10] Tony Kerzmann and Laura Schaefer, System simulation of a linear concentrating photovoltaic system with an active cooling system, *Renewable Energy*, **41**, 254-261 (2012)
- [11] W. M. Kays, M.E. Crawford, and Bernhard Weigand, *Convective Heat and Mass Transfer: Fourth Edition*, New York: McGraw-Hill International Edition 2005, page 106.

6. Acknowledgements

I would like to thank Rensselaer Polytechnic Institute for the resources and professionals that have provided me with an invaluable education that I plan on using throughout the rest of my career as an engineer. I would like to especially thank Dr. Ernesto Gutierrez-Miravete for all his help and patience he provided throughout the completion of this project. Also, this couldn’t have been possible without the financial support of Electric Boat Corporation. Most importantly, I would like to give my upmost thanks to my family and to my wife, Katelyn, for providing endless and unconditional support throughout my education program at RPI.